J. Electrochem. Sci. Eng. **13(2)** (2023) 297-319; http://dx.doi.org/10.5599/jese.1674

Open Access : : ISSN 1847-9286
www.jESE-online.org

Original scientific paper

Electrochemical determination of vitamin B_6 in pharmaceutical and energy drink samples

Gizaw Tesfaye✉, Negussie Negash and Merid Tessema

Department of Chemistry, Addis Ababa University, P. O. Box 1176, Addis Ababa, Ethiopia

Corresponding author: ✉gizawtes@gmail.com

Received: January 24, 2023; Accepted: February 25, 2023; Published: March 1, 2023

Abstract

A simple and low-cost electrochemical sensor based on poly(phenylalanine) and functionnalized multi-walled carbon nanotubes (F-MWCNTs) modified glassy carbon electrode (GCE) was developed for the determination of vitamin B_6 (VB_6). The surface morphology of modified glassy carbon electrodes was investigated with scanning electron microscopy (SEM) and Fourier transform infrared spectroscopy (FTIR). The electrocatalytic activities of the bare and modified electrodes were investigated in the presence of ferri-ferrocyanide redox couple using cyclic voltammetry (CV) and electrochemical impedance spectroscopy (EIS). The exchange current density (j_o = 2462 μA cm^{-2}) and electron transfer rate constant (k^o = 0.002 cm s^{-1}) were calculated using 5 mM $K_3[Fe(CN)_6]$. The electrochemical activity of poly(phenylalanine)/F-MWCNT/GCE towards VB_6 oxidation was investigated using CV. Parameters including the number of electrons transferred (n = 2), number of protons transferred (H^+ = 2), electron transfer coefficient (α = 0.51) and surface concentration of VB_6 (Γ = 0.24 nmol cm^{-2}) were calculated. At the optimal experimental conditions, the oxidation peak current of VB_6 measured by square wave voltammetry (SWV) was found proportional to its concentration in two linear ranges of 0.5 to 20 μM and 20 to 200 μM with a low detection limit (LOD) of 0.038 μM and limit of quantification (LOQ) of 0.125 μM. Finally, the sensor was successfully used to determine VB_6 in soft drink and pharmaceutical formulation samples.

Keywords

Glassy carbon electrode; electro-polymerization; poly(phenylalanine); F-MWCNTs; pyridoxine; electrochemical sensor; real samples

Introduction

Vitamins are nutrients that are essential for normal cell development, energy generation and red blood cell production [1–3]. Furthermore, they are important cofactors of many enzymes in different metabolic processes occurring in the body [3]. Based on their solubility, vitamins are classified as water-soluble vitamins (vitamin B and vitamin C) and fat-soluble vitamins (vitamin A, vitamin D,

vitamin E, and vitamin K) [1]. Water-soluble vitamins are not stored in the body due to easy discharge through urine [2,4]. Furthermore, they cannot be synthesized in the human body [3,5]. Therefore, they must be obtained from dietary sources for normal cell growth. Among the water-soluble vitamins, VB_6 (pyridoxine) (Figure 1A) plays an important role in body metabolism. VB_6 is involved in amino acid metabolism, red cell production, hemoglobin synthesis, gene expression, enzyme-catalyzed reactions and nervous and immune systems [1,5]. VB_6 is found in many foods such as chickpeas, turkey, fish, starchy vegetables, potatoes, bananas, meats, organ meats, fortified cereals and whole grains [6,7]. The recommended dietary allowance (RDA) for VB_6 is 1.3 mg/day for adult males and females and even higher amounts are advised for males and females over the age of fifty years [6]. The normal range of VB_6 in human blood is 5–50 μg L^{-1} [1]. The deficiency of VB_6 causes colorectal cancer, skin problems, weakness, depression, convulsions, neurological diseases, anemia, hyperlipidemia, hypertension, obesity, cardiovascular diseases, mucous membranes and circulatory system problems [1,3]. However, excessive intake of VB_6 for a long time leads to different allergic reactions such as rash, itching, severe dizziness and breathing [2].

It is vital to develop sensitive and selective methods for the quick determination and monitoring of VB_6 in various matrices, such as food and pharmaceuticals, in light of its significance and potential negative effects. For the purpose of determining VB_6, a number of analytical techniques, including liquid chromatography [8], gas chromatography-mass spectrometry [9], chemiluminescence [10], capillary zone electrophoresis [11] and spectrophotometry [12] have been described in the literature. Many of these analytical techniques require tedious and time-consuming procedures and involve highly sophisticated instrumentation and toxic organic reagents [5,13,14]. Due to great selectivity, sensitivity, quick response time, ease of use and low cost, electrochemical methods have received a lot of interest in electroanalysis [4,15]. Furthermore, combined with portable detection equipment, electrochemical methods offer great promise for on-site environmental monitoring [16].

Glassy carbon electrode (GCE) has been widely used as a working electrode for sensor fabrication due to its resistance to chemical attack, easy modification, good reproducible surface, low porosity, high electrical conductivity, wide potential window and good mechanical stability. However, at bare electrode surfaces, VB_6 shows weak or no electrochemical response. In order to increase the rate of electron transfer and lower the overpotential, it is required to change the electrode surface with appropriate modifiers [17]. Various modified electrodes, such as GCE modified with a hybrid of polydopamine and reduced graphene [18], multi-walled carbon nanotube and cobalt phthalocyanine (CoPc) modified pyrolytic graphite electrode [19], NiO-carbon nanotubes (CNTs) nanocomposite and 1-methyl-3-octylimidazolium hexafluorophosphate modified carbon paste electrodes [20], poly(arginine) modified carbon nanotube paste electrode [21], cobalt hexacyanoferrate modified carbon paste electrode [22] and gold nanostructures modified carbon paste electrode [23] have been fabricated for the electrochemical determination of VB_6. However, all these electrodes suffer from tedious modification processes. Therefore, it is important to develop low-cost and simple electrochemical method for the VB_6 determination.

Recently, polymers have received much attention for electrode modification due to their biocompatibility, chemical stability, ease of synthesis, more active sites and low-cost processability [24,25]. The advantages of electrochemical polymerization over chemical polymerization for polymer preparation include homogeneous and stable polymer film formation on the electrode surface, ease of preparation, cost-effectiveness, strong adhesion of the polymer film to the electrode surface and simple control of film thickness by adjusting electrochemical parameters only [25]. Because of their ease of processing, high electrocatalytic capacity, easy interaction with the target analyte *via*

hydrogen bonding or electrostatic interaction caused by the presence of amine and carboxyl groups, stable film forming ability, high biocompatibility and low cost, poly(amino acids) were used extensively as electrode modifiers [26].

Different amino acids have been used to modify electrode surfaces for the electrochemical analysis of various analytes [27-31]. Among the major amino acids, phenylalanine (Figure 1B) is easily electropolymerized on the electrode surface to form poly(phenylalanine) [32]. A number of analytes have been studied electrochemically using electrodes modified with poly(phenylalanine) [33-35]. With respect to the intended analytes, the modified electrode demonstrated high electrocatalytic activity and stability.

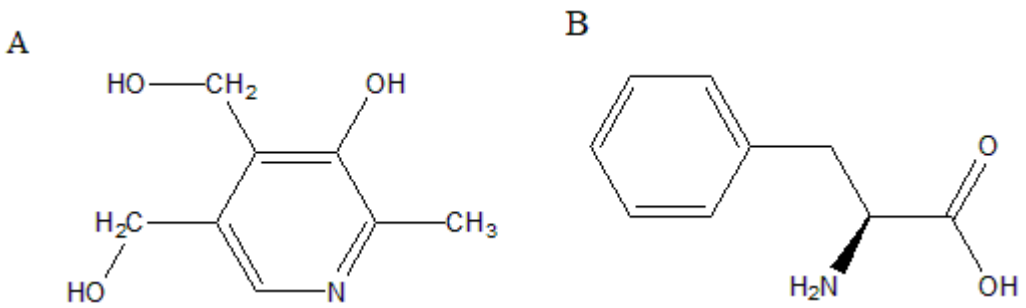

Figure 1. *Chemical structures of (A) VB_6 and (B) phenylalanine*

On the other hand, CNTs modified electrodes have been widely used in electrochemical sensors due to their high electrical conductivity, biocompatibility, ease of functionalization, mechanical strength, high adsorption capacity, chemical stability and high surface area [26,36]. Furthermore, carbon nanotubes are easily incorporated into other materials to produce synergistic effects that increase sensitivity to a target analyte. However, a significant obstacle to the current development of CNT-based devices is the limited solubility of CNT in most solvents. Because of the strong π-π interactions between the aromatic rings, CNTs tend to aggregate in aqueous solutions, making challenging to disperse them and use for development of electrochemical sensors. Therefore, it is important to prepare hydrophilic surface CNTs to overcome the dispersion problem. Functionalization of CNT enhances solubility, processibility and interaction with other materials [37]. CNTs can be covalently functionalized by oxidation with strong acids such as HNO_3, H_2SO_4 or their mixtures [38]. Oxidation of CNTs results in open-ended nanotubes containing oxygenated functional groups such as carboxylic acid, ketone, alcohol and ester groups [38]. The presence of these oxygen-containing functional groups on CNT increases its interaction with a polymer during composite formation [38]. As described in many literature studies, the combination of carbon nanotube with polymer significantly improves the electrocatalytic activity of the modified surfaces compared to individual CNTs or polymer-modified electrodes due to the synergistic effect of CNT and polymer [25,26].

In this study, taking into account the synergistic effect of F-MWCNT and polymer, we constructed an effective and low-cost electrochemical sensor for the determination of VB_6 in food and pharmaceutical samples. The electro-polymerization of phenylalanine on carbon nanotubes is carried out using potentiodynamic polarization. The prepared electrode, poly(phenylalanine)/F-MWCNT/GCE is characterized by Fourier-transform IR (FTIR), scanning electron microscopy (SEM), cyclic voltammetry (CV) and electrochemical impedance spectroscopy (EIS) techniques. The electrochemical behavior of VB_6 at the modified electrode is investigated using CV, while its analytical determination is performed by square wave voltammetry (SWV). The preparation procedures for the F-MWCNT and poly(phenylalanine) modified GCE and sensing mechanism are illustrated in the Graphical abstract.

Experimental

Reagents and chemicals

All chemicals used in this study were analytical grade and were used without any further purification: pyridoxine hydrochloride (VB_6) (≥ 98 %), vitamin B_1 (≥ 99 %), potassium nitrate (99 %), sodium sulfate (≥ 99 %) and ascorbic acid (≥ 99.7 %) were obtained from (BDH, England). Vitamin B_2 (≥ 98 %), L-phenylalanine (99 %), caffeine (99 %), tartaric acid (98 %), acetic acid (99.8 %), glucose (≥ 99.5 %), starch (AR grade), multi-walled carbon nanotube (MWCNT) (> 90 % carbon basis) synthesized by chemical vapor deposition, potassium ferricyanide (99 %), sucrose (≥ 99.5 %), lactose (≥ 99%), vitamin B_{12} (≥ 98 %), vitamin B_9 (≥ 97 %), sodium hydroxide (98 %) and hydrochloric acid (37 %) were obtained from Sigma-Aldrich (USA). Citric acid (99 %), sodium citrate (98 %) and dipotassium hydrogen phosphate (98 %) were obtained from Research–Lab. Chem. Industries (Mumbai, India). Potassium dihydrogen phosphate (98 %), magnesium chloride (99.5%), copper nitrate (98 %), iron(II) nitrate (98 %), sodium carbonate (99.5 %) and sodium bicarbonate (99.7 %) were obtained from Hopkin and Williams LTD (England). Potassium chloride (98 %) was purchased from Riedel-de Haën (France). Boric acid (99.5 %) was obtained from Carlo Erba reagent SPA (Italy).

5 mM stock solution of VB_6 was prepared by dissolving accurately weighed amounts of VB_6 in distilled water. Until use, the stock solution was kept in a refrigerator. A suitable quantity of phenylalanine was dissolved in phosphate buffer solution pH 8.0 to prepare a 2mM phenylalanine solution. Acetate buffer solutions (ABS) were prepared by mixing 0.1 M acetic acid and 0.1 M sodium acetate. 0.1 M NaOH and 0.1 M HCl solution were used to adjust the pH of the solution. The stock solutions were diluted with ABS pH 4.5 to prepare the working solutions.

Apparatus and instruments

Electrochemical experiments, including CV, SWV and EIS were carried out using CHI 760D Electrochemical Workstation (CH Instruments, USA). A three-electrode system consisting of bare GCE or modified GCE (geometric surface area of 0.07 cm^2) as a working electrode, platinum wire as a counter electrode and Ag/AgCl (3 M KCl) as a reference electrode were used. The pH of the solution was measured using a pH meter (sensION, SHA Snilu Instruments Co. Ltd., China). The surface morphology and chemical structure of the modified electrodes were studied using SEM (Cx-200 Coxem, Korea) and FTIR (Spectrum 65 FT-IR (Perkin Elmer, USA) using KBr disk, respectively.

Real sample preparation

Beverage sample

Energy drink samples (predatory energy drink, Ambo mineral water S.C. Ethiopia) were obtained from a nearby supermarket in Addis Ababa, Ethiopia, and kept in a refrigerator until analysis. 100 mL of the liquid sample was transferred into a beaker and degassed in an ultrasonic bath before voltammetric analysis. Then 2.0 mL of the sample was diluted to 10 mL with 0.1 M ABS pH 4.5 solution. The determination of VB_6 in the sample was performed using the standard addition method. The samples were spiked with a stock solution of VB_6 for the recovery test.

Pharmaceutical sample

A commercial sample of the vitamin B complex (N-VIT, Ningbo Shuangwei Pharm.Co., Ltd., China, containing vitamins B_1, B_6 and VB_{12}) was obtained from a local drugstore in Addis Ababa. Five tablets containing 100 mg of VB6 were precisely weighed and ground into a fine powder. An amount equivalent to one tablet was taken in a 50 mL volumetric flask and dissolved in distilled water by

sonicating it for 10 min. Then, the solution was filtered using Whatman filter paper to obtain a clear filtrate and transferred to a 100 mL volumetric flask and the volume was made up to the mark with distilled water. To achieve a final concentration in the range of calibration curve, the sample solution was further diluted with ABS pH 4.5. SWV quantification of VB_6 in the pharmaceutical formulation was carried out by the standard addition method. For the recovery test, the samples were spiked with various concentrations of the standard solution of VB_6.

Functionalization of multi-walled carbon nanotubes

Functionalization of MWCNTs was performed utilizing the acid oxidation method according to the procedure described in the literature with a minor modification [39]. Briefly, 500 mg of pristine MWCNTs was added to 100 mL of a concentrated solution of HNO_3 and H_2SO_4 at a ratio 1:3 (v/v) in a 200 mL conical flask and heated at 80 °C with continuous starring for 5 h. The resulting mixture was diluted with 200 mL of distilled water and filtered. Then, the mixture was thoroughly rinsed with distilled water until the pH of the filtrate reached 7.0. Finally, the functionalized F-MWCNTs were gathered and dried in an oven at 40 °C for 12 h.

Preparation of modified electrodes

The GCE was properly rinsed with double-distilled water after being carefully polished with 0.05 µm alumina slurry on the polishing pad. The electrode was then successively sonicated in distilled water and ethanol for five minutes to remove any remaining polishing agent from the electrode surface. F-MWCNT suspension was made by dispersing 5 mg of F-MWCNT in 5 mL of double-distilled water and sonicating the mixture for 30 minutes. To prepare F-MWCNT modified GCE, 8 µL of an optimal amount of F-MWCNT suspension was drop cast onto the cleaned GCE and allowed to dry for five minutes in the open air. Then, electro-polymerization was carried out by cyclic voltammetry in the potential range −1.5 to 2.5 V at a scan rate of 0.05 V s^{-1} for 5 cycles in 0.1 M phosphate buffer solution pH 8.0 containing 2 mM phenylalanine. To remove unreacted monomers, the fabricated poly(phenylalanine)/F-MWCNT/GCE was rinsed with double distilled water and dried for five minutes at room temperature. For comparison purposes, poly(phenylalanine)/GCE and F-MWCNT were also prepared with the same procedures described above.

Results and discussion

Construction of poly(phenylalanine)/F-MWCNT/GCE

Poly(phenylalanine) film was deposited on the surface of bare GCE and F-MWCNT/GCE by electrochemical polymerization of phenylalanine using 5 cycles of CV in the potential range −1.5 to 2.5 V at the scan rate of 0.05 V s^{-1} in 0.1 M phosphate buffer solution (pH 8) containing 2 mM phenylalanine monomer. The mechanism of electro-polymerization of phenylalanine was- already reported [40]. The cyclic voltammograms (CVs) for the electro-polymerization of phenylalanine are displayed in Figure 2. In the forward scan, the phenylalanine monomer oxidation peak was observed at 1.6 V, corresponding to the formation of monomer radical due to the oxidation of the amino functional group of phenylalanine. During the reverse scan, the cathodic peak at −0.50 V was observed, corresponding to phenylalanine reduction. The monomer cation radicals can form carbon-nitrogen linkages on the surface of the carbon electrode [28,30]. The deposition of the polymer film on the electrode surface is demonstrated by an increase in the anodic and cathodic peak currents with increasing cycle numbers [28]. After a few cycles, the anodic and cathodic peak currents remain almost stable, indicating that the formation of a polymer film has reached the level

of saturation. A blue coating was noticed on the electrode surface after washing with distilled water, indicating the formation of poly(phenylalanine) film [30]. Scheme 1 describes the electro-polymerization mechanism of phenylalanine.

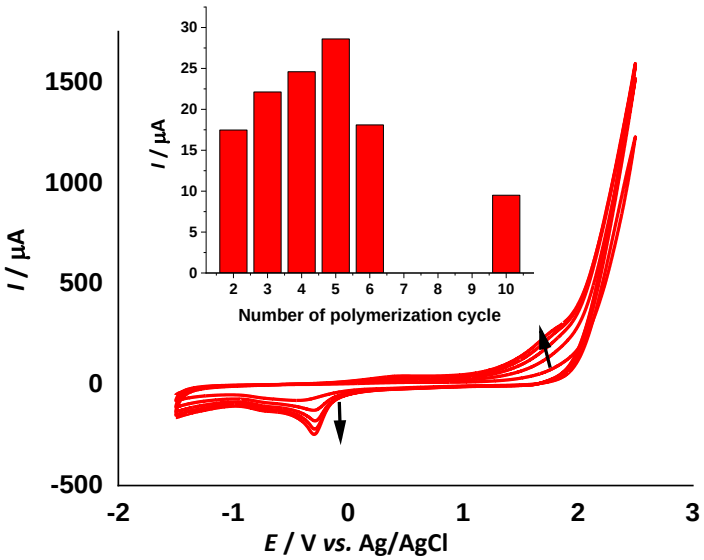

Figure 2. *CVs of electro-polymerization of 2mM phenylalanine in 0.1 M phosphate buffer solution (pH 8.0) on F-MWCNT/GCE surface in the potential range −1.5 and 2.5 V for 5 cycles at a scan rate of 0.05 V s^{-1}. Inset: peak current of 200 µM VB_6 versus the number of polymerization cycles*

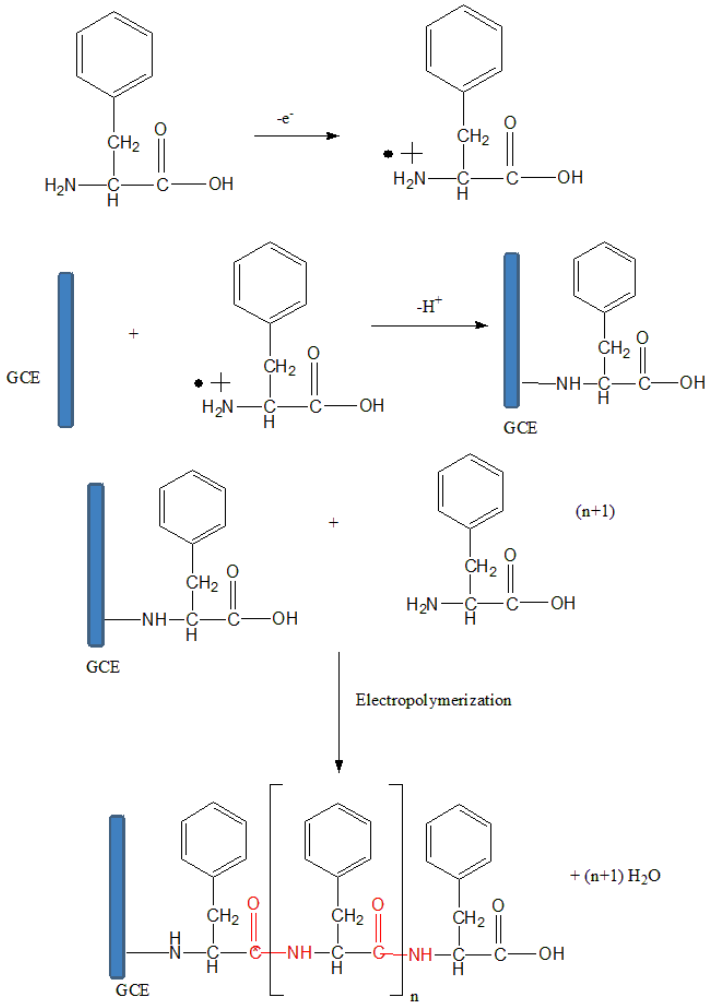

Scheme 1. *Mechanism of electro-polymerization of phenylalanine*

The thickness of the polymer film has an impact on the electrocatalytic capability of the prepared electrode [41]. Therefore, the effect of the number of cycles of electro-polymerization on the electrocatalytic activity of the prepared electrode was examined from 3 to 15 cycles. Due to an increase in active sites at the electrode surface, the peak current of VB_6 increased along with the number of cycles up to 5 cycles (inset of Figure 2). After 5 cycles, the thickness of the polymer film increased and blocked the electron transfer between the electrode and VB6. Thereby, 5 potential scans were chosen to electropolymerize phenylalanine on the electrode surface.

Electrochemical properties of bare and modified GCE

The electrochemical behavior of the bare GCE and modified electrodes were examined by CV and EIS in 0.1 M KCl with 5 mM $[Fe(CN)_6]^{3-/4-}$ taken as a redox probe. The CV responses of bare GCE (curve a), F-MWCNT (curve b), poly(phenylalanine)/GCE (curve c) and poly(phenylalanine)/F-MWCNT/GCE (curve d) are shown in Figure 3. Weak redox peaks and a broad voltammogram were observed for bare GCE (curve a) in comparison to the modified electrodes. Due to the high surface area and conductivity of F-MWCNT, the modification of bare GCE with F-MWCNT enhanced the current response of $[Fe(CN)_6]^{3-/4-}$ and lowered the peak-to-peak potential separation. After electro-depositing poly(phenylalanine) on the GCE, the redox peak current increased and peak-to-peak potential separation reduced because the high conductivity of polymer and more active sites made it easier for $[Fe(CN)_6]^{3-/4-}$ to reach the electrode surface. Similar to this, after F-MWCNT/GCE was modified with poly(phenylalanine), the redox peak currents increased further, and the peak-to-peak separation decreased because of the synergistic effect of F-MWCNT and poly(phenylalanine) for the electron transfer between $[Fe(CN)_6]^{3-/4-}$ and poly (phenylalanine)/F-MWCNT/GCE. Using Randles-Ševčik equation, the electroactive surface areas of the unmodified GCE and modified GCE were estimated [27,42]:

$$I_p = (2.69\times10^5)\, AD^{1/2}z^{3/2}\nu^{1/2}C \quad (1)$$

where I_p / A is peak current, z is a number of electrons involved in the reaction (z = 1), A / cm^2 is electrode active surface area, D (7.6×10^{-6} cm^{2}s^{-1}) is diffusion coefficient of ferricyanide ions in 0.1 M KCl solution, C is the concentration of $K_3[Fe(CN)_6]$ (mmol cm^{-3}) and ν/ V s^{-1} is scan rate.

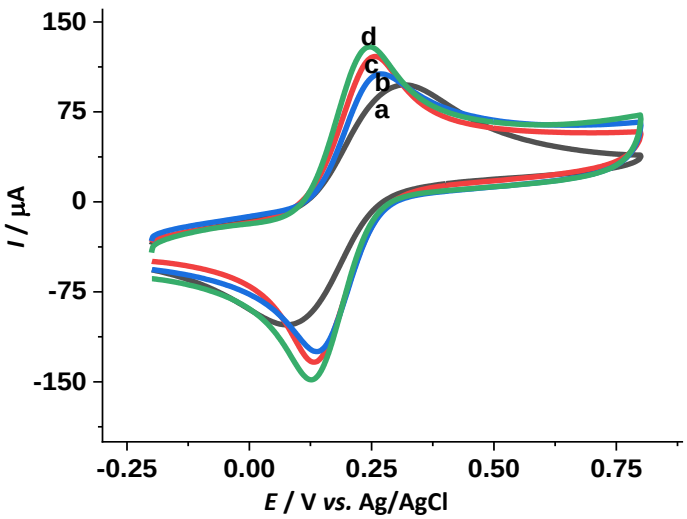

Figure 3. *CVs (ν = 0.1 V s^{-1}) of 5.0 mM $[Fe(CN)_6]^{3-/4-}$ in 0.1 M KCl at: bare GCE (a), F-MWCNT/GCE (b), poly (phenylalanine)/GCE (c) and poly(phenylalanine)/F-MWCNT/GCE (d)*

According to the scan rate analysis, the anodic and cathodic peak currents of all electrodes were found to be proportional to the square root of the scan rate in the range 0.025 to 0.4 V s^{-1}. From the

slopes of I_p versus $\nu^{1/2}$, plots, the electroactive surface area was calculated for each electrode. The calculated values were 0.05, 0.08, 0.09 and 0.12 cm^2 for bare GCE, F-MWCNT/GCE, poly(phenylalanine)/GCE and poly(phenylalanine)/F-MWCNT/GCE, respectively.

Electrochemical impedance spectroscopy (EIS) was used to further examine electrochemical characteristics of unmodified and modified electrodes. Important information about the kinetics of electron transfer at the electrodes can be provided by EIS [43]. In Nyquist plots, the semicircle diameter refers to the electron transfer resistance (R_{ct}) at the electrode surface [44]. Figure 4A shows Nyquist plots of EIS for all electrodes in 0.1M KCl containing 5.0 mM $[Fe(CN)_6]^{3-/4-}$ redox probe. In comparison to other modified electrodes, bare GCE exhibited the highest charge transfer resistance (R_{ct}) and the lowest double-layer capacitance (C_{dl}) value, as shown in Table 1. It was evident that the F-MWCNT modified surface has higher conductivity and surface area than bare GCE since the R_{ct} value of the F-MWCNT/GCE was lower than that of bare GCE. Electrodeposition of poly(phenylalanine) on the surface of bare GCE can also reduce the R_{ct} value by accelerating the electron transfer rate due to its high electrocatalytic ability. Poly(phenylalanine)/F-MWCNT/GCE exhibits the lowest R_{ct} and the highest C_{dl} compared to all other electrodes. The high value of C_{dl} at poly(phenylalanine)/F-MWCNT/GCE indicates the increase in the surface area of the electrode after modification. Thus, more ions transfer from the solution to the electrical double layer, increasing the electrical double layer capacitance. Similarly, Bode plots (Figure 4B, C) revealed that MWCNT or poly(phenylalanine) modified electrode has lower charge transfer resistance (lower impedance at all frequencies) than bare GCE. Poly(phenylalanine)/F-MWCNT modified electrode exhibited the lowest charge transfer resistance. At very high frequencies where solution resistance (R_s) dominates, the impedance values are almost similar for all electrodes. This suggests that modifiers did not have any significant impact on the solution resistance value. Therefore, the combination of MWCNT and poly(phenylalanine) increases exclusively the electron transport between the electrode and $[Fe(CN)_6]^{3-/4-}$. In light of this, the EIS results confirm the CV results. Furthermore, the exchange current density (jo) and electron transfer rate constant (k^o) for the electrodes were computed from the EIS data using the following equations [45]:

$$j_0 = \frac{RT}{zR_{ct}AF} \tag{2}$$

$$k^o = \frac{RT}{R_{ct}ACF^2} \tag{3}$$

where j_0 / A cm^{-2} is the exchange current density, k^o / cm s^{-1} is the electron transfer rate constant, R is the universal gas constant (8.314 J K^{-1} mol^{-1}), T is the temperature (298 K), F is Faraday constant (96485 C mol^{-1}), R_{ct} / Ω is the electron transfer resistance, A / cm^2 is the electrode surface area and z is the number of electrons involved in the reaction (z = 1). The j_0 and k^o values obtained for the bare GCE, F-MWCNT/GCE, poly(phenylalanine)/GCE and poly (phenylalanine)/F-MWCNT/GCE are listed in Table 1.

Table 1. *Electron transfer rate constant, exchange current density, charge transfer resistance and double layer capacitance for bare and modified GCE*

Electrode	k^o / cm s^{-1}	J_0 / μA cm^{-2}	R_{ct} / Ω	C_{dl} / μF
GCE	0.0034	1633	314.4	1.22
MWCNT/GCE	0.0043	2100	152.8	1.62
poly(phenylalanine)/ GCE	.0046	2246	127	2.45
poly(phenylalanine) /F-MWCNT/GCE	0.0051	2462	86.91	16.0

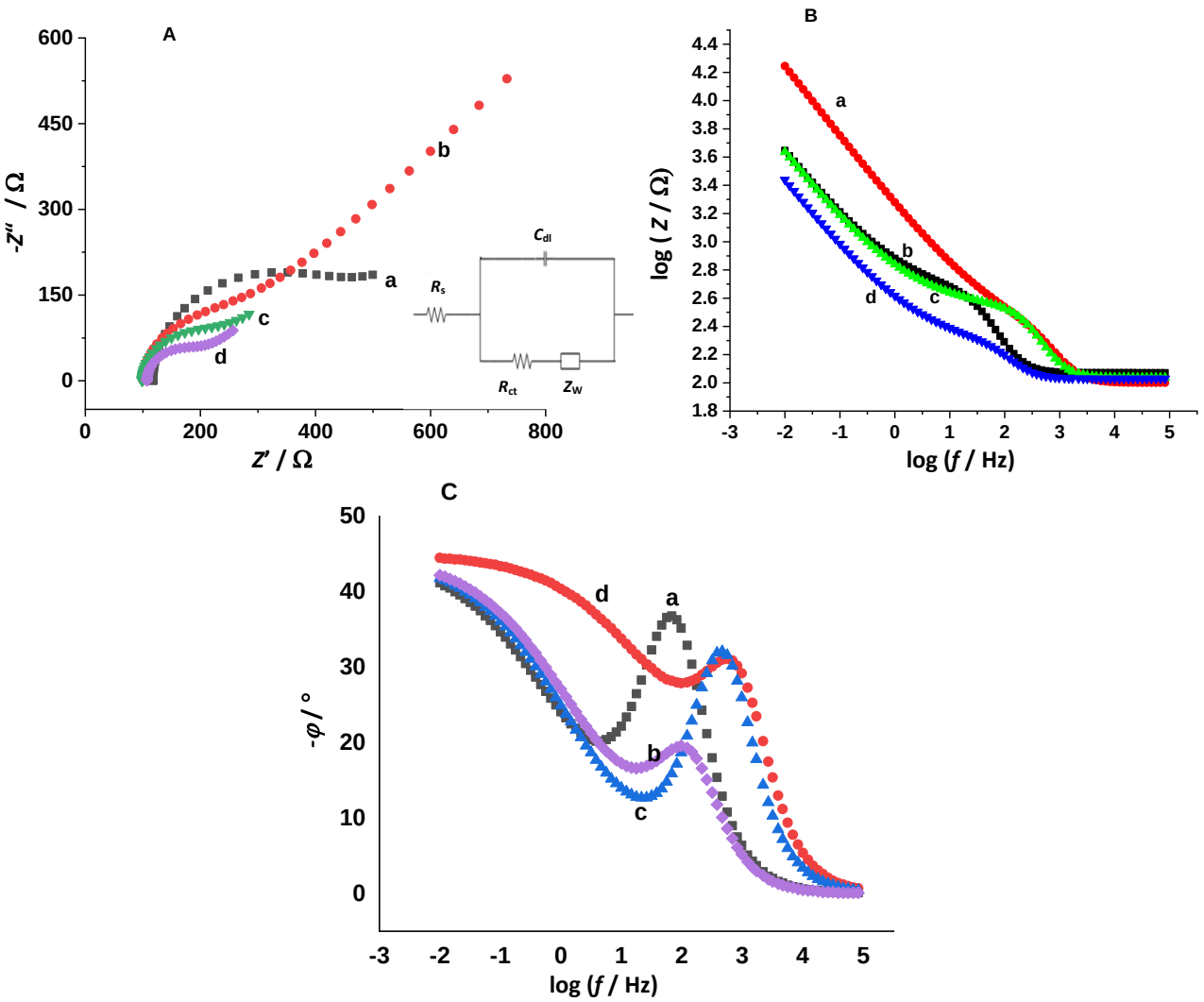

Figure 4. *(A) Nyquist plots of 5.0 mM $[Fe(CN)_6]^{3-/4-}$ in 0.1 M KCl at: bare GCE (a), F-MWCNT/GCE (b), poly (phenylalanine)/GCE (c) and poly(phenylalanine)/F-MWCNT/GCE (d). Inset: Randles equivalent electrical circuit used for fitting Nyquist plots; R_s is solution resistance, R_{ct} is charge transfer resistance, C_{dl} is double layer capacitance, and Z_w is diffusion (Warburg) impedance. (B) Bode plots, log Z vs. log frequency and (C) phase angle vs. log frequency at bare GCE (a), F-MWCNT/GCE (b), poly(phenylalanine)/GCE (c) and poly(phenylalanine)/F-MWCNT/GCE (d). Frequency range of 100 kHz–0.1 Hz, applied potential of 0.15 V and amplitude of 0.005 V*

The findings demonstrated that greater j_0 and k^o values were achieved for the composite modified electrode, poly(phenylalanine)/F-MWCNT/GCE, due to its large surface area and presence of additional functional groups that were active and facilitated the transport of electrons between the electrode and $[Fe(CN)_6]^{3-/4-}$. It seems that the electron transfer process is simpler and quicker at the composite-modified electrode.

Surface characterization

FTIR was used to investigate the surface functional groups of functionalized MWCNT and the deposition of polymer film on the electrode surface. Figure 5 shows FTIR spectra of pristine MWCNT, F-MWCNT and poly (phenylalanine)/F-MWCNT. It could be seen that the F-MWCNT exhibited new bands compared to pristine MWCNT due to the attachment of new functional groups on their surface. The FTIR spectrum of MWCNT showed weak peaks at 3430 and 1646 cm^{-1} corresponding to O–H stretching vibration of the C–OH, which can be introduced during their synthesis and conjugated C=C stretching vibration of pristine MWCNT, respectively. Absorption bands at 2918 and

2853 cm^{-1} are assigned to asymmetric and symmetric stretching vibrations of the C–H [46]. For F-MWCNT, a strong absorption band observed at 3445 cm^{-1} is attributed to OH stretching vibration of the –COOH groups [39,46]. The absorption bands at 2927 and 2862 cm^{-1} are assigned to asymmetric and symmetric stretching vibrations of the C–H bond in CH_2 of F-MWCNT, respectively [46]. A weak band at 1749 cm^{-1} is assigned to the stretching vibration of C=O of the carboxyl group [39]. The absorption peak at about 1639 cm^{-1} is assigned to the C = C skeletal stretching vibration of F-MWCNT. The band at 1447 cm^{-1} is assigned to C-H bending vibration of $–CH_2$ [46]. The peak at 1380 cm^{-1} corresponds to O–H bending vibration [39]. The absorption band at about 1083 cm^{-1} can be ascribed to the C–O stretching vibrations of epoxy groups [46]. The increase in the intensity of O–H stretching vibration and formation of C=O and C–O functional groups after oxidation of pristine MWCNT indicate successful functionalization of MWCNT [39]. The structural properties of poly(phenylalanine) /F-MWCNT have also been investigated using FTIR spectroscopy. The absorption band at 3443 cm^{-1} corresponds to O–H stretching of MWCNT and the N–H stretching of poly (phenylalanine) [47]. The peaks at 2922 and 2852 cm^{-1} are attributed to asymmetric and symmetric stretching vibrations of the C–H in CH_2 [47]. The characteristic band at 1738 cm^{-1} is assigned to the stretching vibration of C=O of the carboxylic group. The band at 1634 cm^{-1} is attributed to the C=O stretching vibration of the amide group on the poly (phenylalanine) [47]. The band at 1465 cm^{-1} is attributed to C–H bending vibration of the CH_2 groups and phenyl ring stretching. The band observed at 1383 cm^{-1} is assigned to O–H bending vibration and phenyl ring stretching [39]. The band at 1226 cm^{-1} is due to C–N stretching of secondary amine. The peak observed at 1081 cm^{-1} is assigned to C–O stretching of the alkoxy group and C–H bending in the phenyl ring [46]. The results obtained from the FTIR spectrum indicated the successful functionalization of MWCNT and deposition of the polymer film.

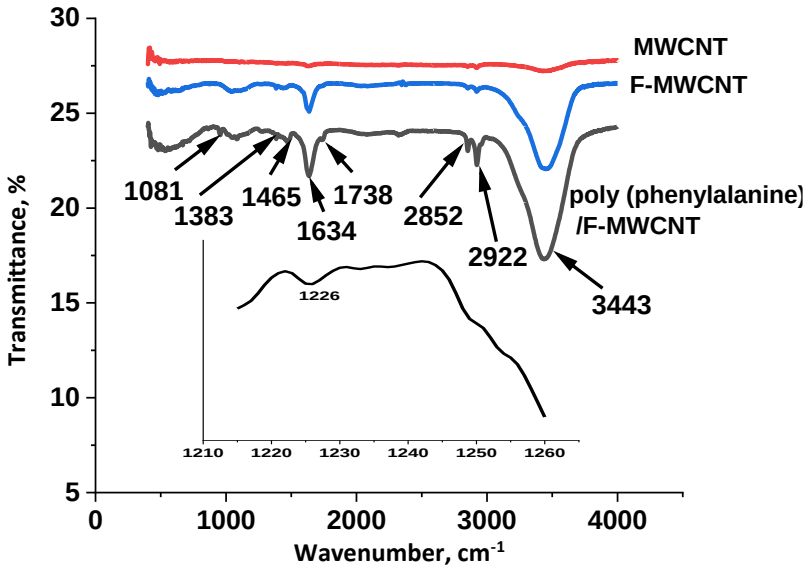

***Figure 5**. FTIR spectra of MWCNT, F-MWCNT and poly(phenylalanine) /F-MWCNT*

The morphologies of bare GCE, F-MWCNT/GCE, poly(phenylalanine)/GCE and poly(phenylalanine)/F-MWCNT/GCE were investigated by SEM. As shown in Figure 6A, bare GCE has a smooth surface structure. After the deposition of F-MWCNT on GCE, porous and thread-like structures of F-MWCNT were observed (Figure 6B). Figure 6C shows a loose and rough surface of poly (phenylalanine) film on GCE. After the deposition of poly(phenylalanine) on F-MWCNT (Figure 6D), a dense and tight surface structure of poly(phenylalanine) film is observed on F-MWCNT, providing

supplementary surface area for adsorption of VB_6. The π-π interaction and hydrogen bonding between F-MWCNT and poly(phenylalanine) were strong enough to make the polymer film attached to F-MWCNT. This strong interaction between F-MWCNT and poly (phenylalanine) results in high stability of the composite material. The results obtained from the SEM study reveal the successful deposition of F-MWCNT on bare GCE and the uniform deposition of poly(phenylalanine) on F-MWCNT.

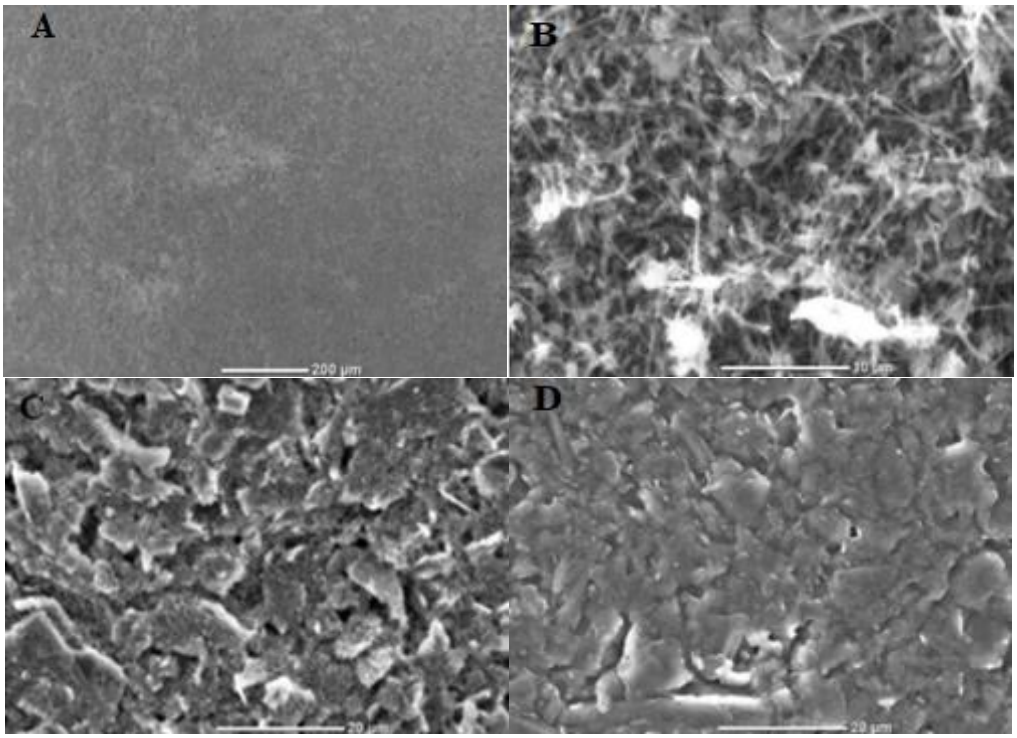

Figure 6. *SEM images of bare GCE (A), MWCNT/GCE (B), poly (phenylalanine/GCE (C) and poly(phenylalanine) /MWCNT/GCE (D)*

Cyclic voltammetric performance of VB_6 at bare and modified GCE

The electrochemical behavior of VB_6 at bare GCE and modified GCE was studied by CV at the scan rate of 0.1 V s^{-1} in ABS pH 4.5. Figure 7 shows CVs of 200 µM VB_6 at GCE (curve a), F-MWCNT/GCE (curve b), poly(phenylalanine)/GCE (curve c) and poly(phenylalanine)/F-MWCNT/GCE (curve d). At the bare GCE (curve a), VB_6 shows a weak oxidation peak indicating slow electron transfer kinetics. Compared to bare GCE, an increase in peak current and decrease in peak potential are observed at F-MWCNT/GCE due to the presence of oxygen-containing functional groups and high conductivity of F-MWCNT which facilitate the accumulation of VB_6 and electron transfer rate at the surface of the electrode. At poly (phenylalanine)/GCE, oxidation peaks higher than the bare GCE and F-MWCNT/GCE were observed. The enhanced peak current observed at poly(phenylalanine)/F-MWCNT/GCE indicates the enhanced kinetics of the electrochemical reaction due to the synergistic effect of MWCNT and poly(phenylalanine), such as high conductivity and presence of functional groups, which facilitate the accumulation of VB_6 through hydrogen bonding and π-π interaction (Scheme 2). Furthermore, the deposition of F-MWCNT and poly(phenylalanine) onto the GCE provide more conducting pathways (more active sites) to ease the electron transfer between the surface of the electrode and the analyte. In the reverse scan, no cathodic peak was observed at all the electrodes, indicating that the electrochemical oxidation of VB_6 is irreversible [22].

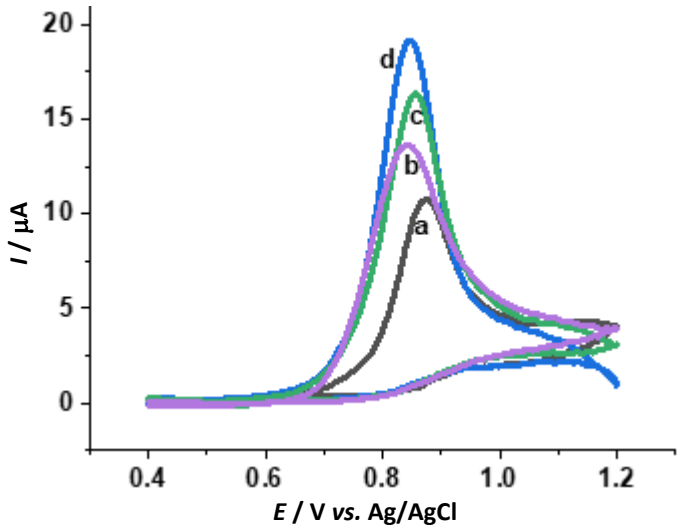

Figure 7. *CVs (0.1 Vs^{-1}) of bare GCE (a), F-MWCNT/GCE (b), poly(phenylalanine)/GCE (c), poly(phenylalanine) /F-MWCNT/GCE (d) (background subtracted) in the presence of 200 µM VB_6 in 0.1 M ABS pH 4.5 after accumulation at 0.0 V for 120 s*

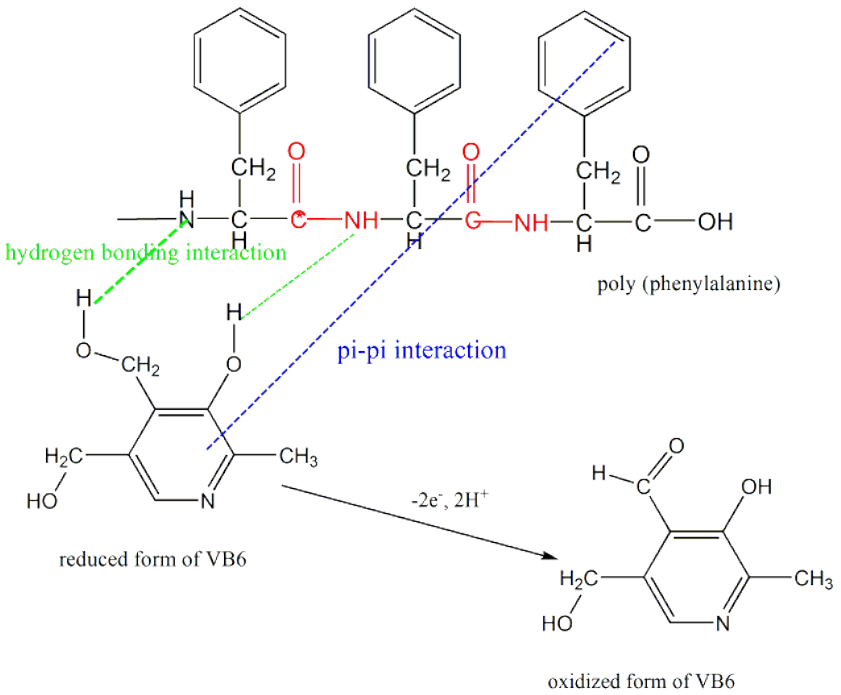

Scheme 2*. Possible interaction of VB_6 with poly(phenylalanine)/F-MWCNT modified electrode and its mechanism of electrooxidation*

The performance of the sensor was examined to determine the impact of the order of deposition of F-MWCNT and polymer. The electrocatalytic activity for the oxidation of VB_6 was found to be higher when F-MWCNT is deposited on the GCE before phenylalanine polymerization (poly(phenylalanine)/F-MWCNT/GCE), as opposed to the case when phenylalanine polymerization was followed by F-MWCNT deposition (F-MWCNT/poly(phenylalanine)/GCE). It is likely that the superior performance of poly(phenylalanine)/F-MWCNT/GCE is caused by the increased surface area when F-MWCNT was applied first. This makes it easier to apply poly(phenylalanine) and increases the number of active sites on the electrode surface [48]. Additionally, it was examined how well the poly(phenylalanine)/F-MWCNT/GCE worked during successive measurements. The oxidation peak current was not considerably altered after 10 SWV measurements of 200 µM VB_6 solution, demonstrating high operational stability of the modified electrode.

Optimization of experimental conditions

Effect of amount of F-MWCNT

SWV was used to examine how the amount of F-MWCNT affected the sensitivity of VB_6. To get optimum amount of F-MWCNT, different amounts of F-MWCNT were dropped onto GCE. Increasing the amount of F-MWCNT up to 8 µL improved the current response of VB_6. However, the sensitivity was reduced at volumes greater than 8 µL. This is explained by the thickening of the F- MWCNT layer, which interferes with electron transfer and decreases electrocatalytic activity. Therefore, 8 µL was selected as the optimum amount of F-MWCNT for the preparation of the sensor electrode.

Impact of solution pH

CV measurements were made in the pH range of 3.0 to 7.0 to determine how the pH of ABS affects the current response of 200 µM VB_6 at poly(phenylalanine)/F-MWCNT/GCE (Figure 8A). The peak current of VB_6 increased progressively from pH 3.0 to 4.5, as shown in Figure 9B, and then fell gradually with increasing pH. From the fact that pKa values of VB_6 are $pKa_1 = 5$ and $pK_{a2} = 8.96$ [4,49] while p*K*as of phenylalanine are $pK_{a1} = 2.47$ and $pK_{a2} = 9.13$ [32], the increase in current response with pH from 3.0 to 4.5 might be due to the increase in electrostatic attraction between the positively charged VB_6 (pH < 5.0) and negatively charged polymer film (pH >2.47). The charge density on both VB_6 and poly (phenylalanine) increases as the pH rises, which causes the electrostatic attraction between VB_6 and poly (phenylalanine) to decrease. This reduces the accumulation of VB_6 at the electrode surface. Thus, 0.1 M ABS pH 4.5 was chosen as the appropriate supporting electrolyte for subsequent investigations.

Furthermore, the pH of the solution also affects the oxidation peak potential of VB_6. The anodic peak potential shifted negatively with the increasing pH of the solution, demonstrating that peak potential is dependent on solution pH. The oxidation peak potential of VB_6 changed linearly with the solution pH in the range 3.0 to 7.0. The regression equation for the dependence of the peak potential on the pH is given by the equation (Figure 8B): $E_p = -0.063$ pH +1.18 ($R^2 = 0.994$). The slope is close to the Nernstian value of −59 mV, indicating the same number of protons and electrons are involved in the electrochemical oxidation of VB_6, which is in agreement with previous works [4,5,20].

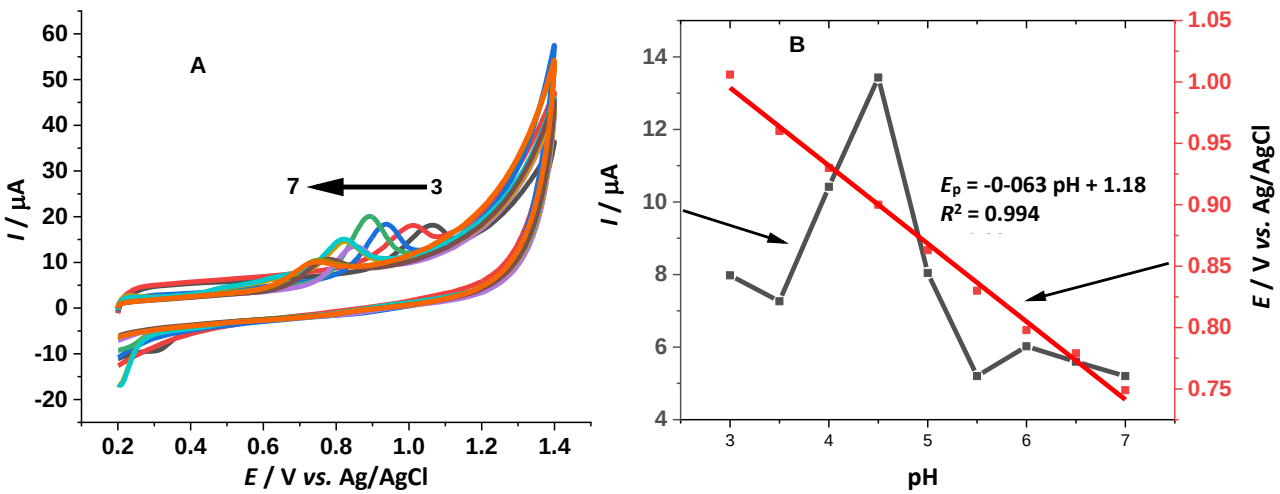

***Figure 8**. (A) CVs of 200 µM VB_6 at poly (phenylalanine)/F-MWCNT/GCE in 0.1 M ABS of various pH values (3.0, 3.5, 4.0, 4.5, 5.0, 5.5, 6, 6.5 and 7) at scan rate of 0.1 V s^{-1}. (B) Effect of pH on the peak current and peak potential values of VB_6*

Scan rate study

By using cyclic voltammetry, the influence of scan rate on the oxidation peak current and peak potential of 200 M VB_6 in ABS pH 4.5 at the poly(phenylalanine)/F-MWCNT/GCE was investigated in order to determine the electrochemical reaction mechanism of VB_6 at the modified electrode (Figure 9A). As shown in Figure 9B, the oxidation peak current is proportional to the scan rate in the range 0.025 to 0.3 V s^{-1}. According to regression equations I_{pa} = 112.6 + 1.08 (R^2 = 0.998), the electro-oxidation of VB_6 at the surface of the modified electrode is adsorption controlled [15]. The relationship between the logarithm of peak current (log *I*) and the logarithm of scan rate (log υ) in the range 0.025 to 0.3 V s^{-1} was further investigated. As shown in Figure 9C, there is good linearity between log *I* and log υ. The corresponding regression equations is: log I_{pa} = 0.89 log ν + 1.98 (R^2 = 0.996) with a slope close to the theoretical value of 1, confirming the electrochemical oxidation of VB_6 at poly (phenylalanine)/F-MWCNT/GCE as a surface-controlled process. Moreover, the influence of scan rate on the peak potential of VB_6 was studied. With increasing scan rate, the oxidation peak potential of VB_6 shifted to a more positive value, indicating that the electrooxidation of VB_6 at poly(phenylalanine)/ /F-MWCNT/GCE is irreversible [20]. The linear regression equations for the variation of the oxidation peak potential (*E*p) with the logarithm of scan rate (log υ) in the range 0.025 to 0.3 V s^{-1} is given by the equation: E_{pa} = 0.052 log ν - 0.93, R^2 = 0.996 (Figure 9D).

According to Laviron's equation [50,51], the relationship between E_p and log *v* for an irreversible electrode reaction is given by:

$$E_p = E^o + \frac{2.303RT}{\alpha zF}\log\frac{RTk}{\alpha zF} + \frac{2.303RT}{\alpha zF}\log\nu \tag{4}$$

where E^o is the formal potential, *T* is the temperature (298 K), *α* is the transfer coefficient, *z* is the number of electrons transferred, ν is scan rate, *F* is Faraday's constant (96,480 C mol^{-1}), *R* is the universal gas constant (8.314 J mol^{-1} K^{-1}), and *k* is the heterogeneous electron-transfer rate constant. From the plot of E_p versus log ν, the slope 2.303*RT*/ *αzF* equals 0.052. Using this value, αn was calculated to be 1.12. For an irreversible electrode reaction [51], α can be given as:

$$\alpha = \frac{47.7}{E_{pa} - E_{pa/2}} \tag{5}$$

where $E_{pa/2}$ is the potential where the current is half the peak value. Thus, from eq. (5) *α* was found to be 0.51. Additionally, it was determined that 2.2 (~2) electrons were involved. Thus, the oxidation of VB_6 requires two electrons [5,18]. From the relationship between E_{pa} and pH, an equal number of electrons and protons are transferred during the electrooxidation of VB_6. Therefore, the electrode reaction mechanism for VB_6 oxidation at poly(phenylalanine)/F-MWCNT/GCE involves two electrons and two protons. Furthermore, it is possible to determine the surface concentration of VB_6 at poly (phenylalanine)/F-MWCNT/GCE from the slope of the linear plot of oxidation peak current *vs. v* using the following equation [52]:

$$I_{pa} = \frac{z^2F^2\Gamma A\nu}{4RT} \tag{6}$$

where Γ / mol cm^{-2} is the surface concentration of electroactive species, *A* / cm^2 is the electrode surface area and *z*, *F*, ν, *R*, and *T* are as described in Eq. (4). The surface coverage of VB_6 at the poly(phenylalanine)/F-MWCNT/GCE was calculated to be Γ = 0.24 nmol cm^{-2}.

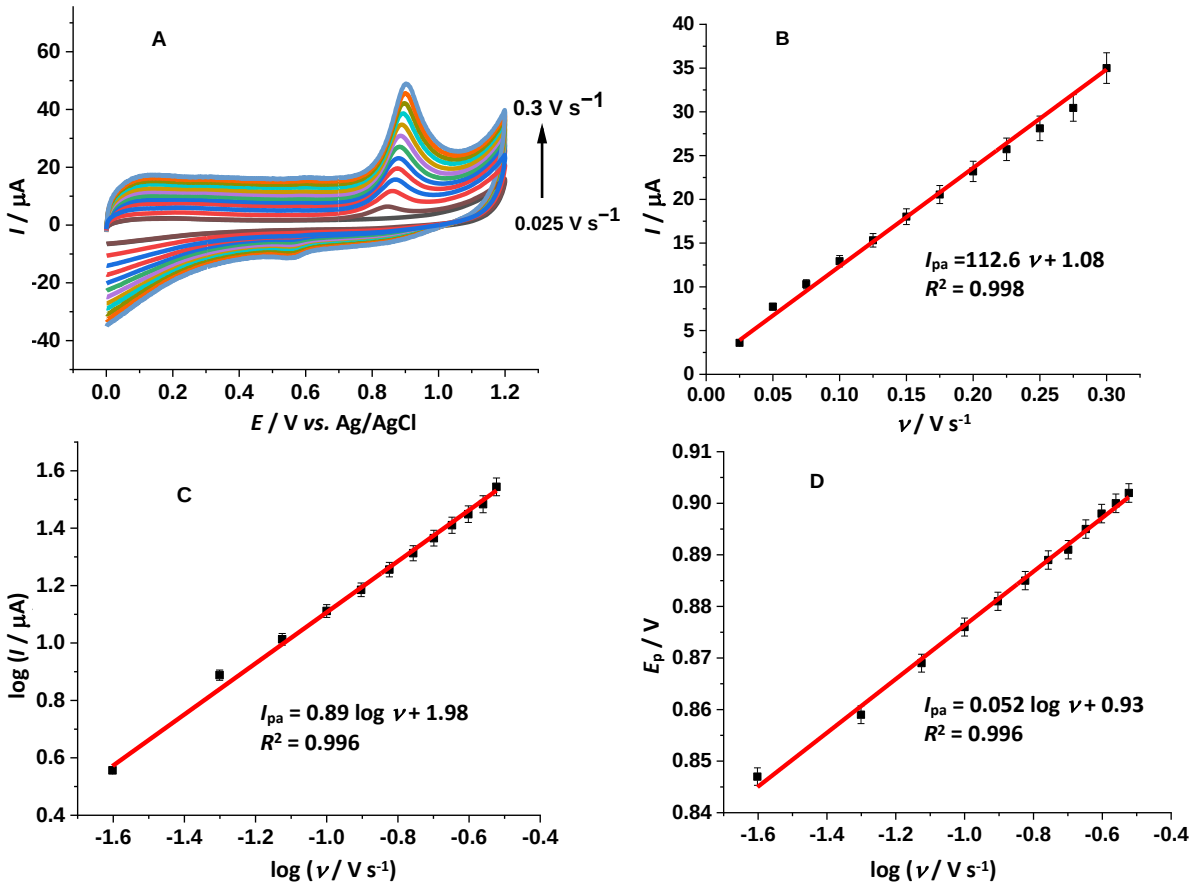

Figure 9. *(A) CVs of 200 µM VB_6 at poly (phenylalanine)/F-MWCNT/GCE in ABS pH 4.5 at scan rates of 0.025, 0.05,0.075, 0.1, 0.125, 0.15, 0.175, 0.2, 0.25, 0.3, 0.350, 0.4 V s^{-1}. (B) Plot of the oxidation peak current versus scan rate (ν). (C) Variation of the logarithm of the oxidation peak current (log I) with the logarithm of scan rate (log ν). (D) Variation of the oxidation peak potential (E_p) with the logarithm of scan rate (log ν)*

Determination of VB_6 at poly(phenylalanine)/F-MWCNT/GCE

Square wave voltammetry (SWV) determination of VB_6 was performed under the optimized experimental conditions in ABS pH 4.5 in the potential range 0 to 1.2 V. According to Figure 10A, the peak currents increased linearly from 0.5 to 200 M of VB_6 concentration.

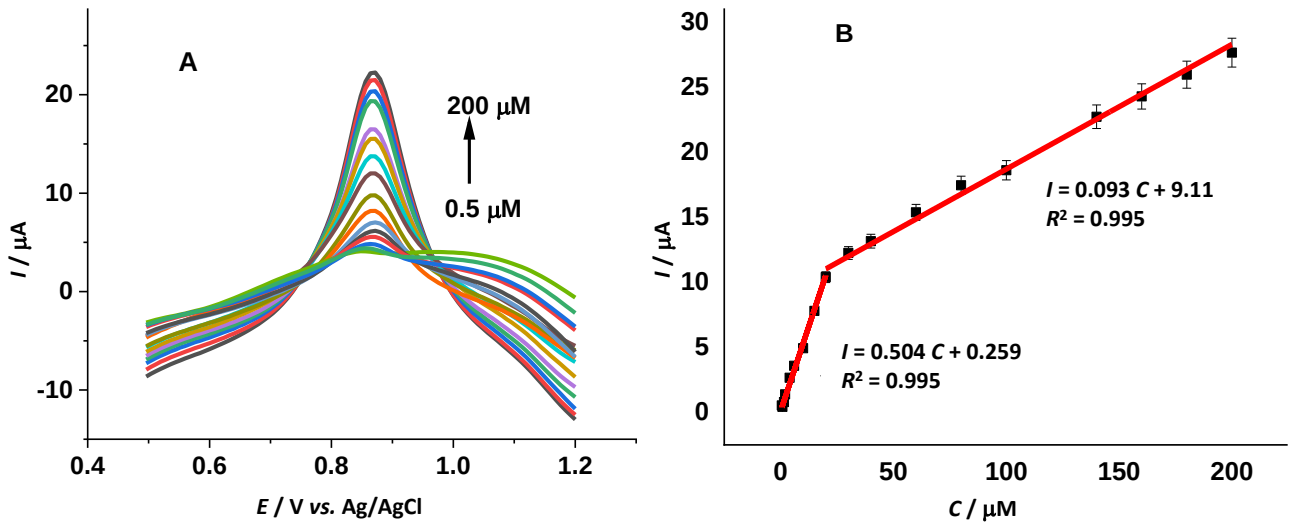

Figure 10. *(A) SWVs for different concentrations of VB_6: 0.5, 0.8, 1.5, 2, 4, 6, 10, 20, 30, 40, 60, 80, 100, 140, 160, 180 and 200 µM in 0.1 M ABS pH 4.5. (B) Plot of the peak current versus concentration of VB_6 at poly(phenylalanine)/F-MWCNT/GCE. Conditions: E_{acc}, 0.0 V; t_{acc}, 120 s. SWV parameters: frequency = 35 Hz; step potential = 8 mV and pulse amplitude = 40 mV*

Two linear ranges could be seen on the VB_6 calibration curve. The first linear range is 0.5 to 20 µM and the second is 20 to 200 µM with regression equations: $I = 0.504\ C + 0.259$, $R^2 = 0.995$ and $I = 0.093\ C + 9.11$, $R^2 = 0.995$, respectively (Figure 10B). Error bars are added to the graph using the standard deviation of triplicate measurements of each data point. LOD and LOQ limits were calculated from the oxidation peak current of VB_6 using the following equations: LOD = $3s/m$ and LOQ = $10s/m$, where s is the standard deviation of the oxidation peak currents ($n = 3$) of the lowest concentration in the linear range and m is the slope of the calibration curve. The calculated LOD and LOQ values are 0.038 and 0.125 µM, respectively. Furthermore, the linear range and detection limit obtained in this study were compared with the results of previously reported electrochemical methods for the determination of VB_6 (Table 2). The findings suggest that the proposed sensor exhibits a better linear range and detection limit than most of the reported sensors. The proposed sensor is also inexpensive and easy to make.

Table 2. *Comparison of reported analytical data for VB_6 determination obtained by sensor electrodes*

Modified electrode	Technique	Concentration linear range, µM	LOD, µM	Ref.
[a]P-doped/PGE	[l]DPV	0.5–300	0.065	[4]
[b]44-DABP/GCE	DPV	15.7–2210	4.7	[5]
[c]AuNps/POAP/PGE	DPV	5–200	0.30	[1]
[d]PMG/fCNT/CE	DPV	100–800	9.4	[53]
[e]Au-CuO/MWCNTs/GCE	DPV	0.79–18.4	0.15	[54]
[f]CrHCF/GCE	CV	1.33–13.2	0.035	[55]
[g]NiZCB-GCE	DPV	0.3–5.9	0.09	[49]
[h]MWCNT/CoPc/PGE	DPV	10–400	0.5	[19]
[i]CoHCF/MCPE	SWV	5–26	0.17	[22]
[j]N,S-GQD-CS/ GCE	SWASV	0.1–18	0.03	[56]
[k]ePADs	SWV	200–2000	29.5	[57]
poly(phenylalanine)/F-MWCNT/GCE	SWV	0.5–20 and 20–200	0.038	This work

[a]Phosphorus-doped pencil graphite electrode; [b]4,4'-diamino benzophenone modified glassy carbon electrode; [c]gold nanoparticles and non-conducting polymeric film of o-aminophenol; [d]poly(methylene green) (PMG)and functionalized carbon nanotubes (fCNT) modified graphite composite electrode (CE); [e]copper oxide (shell) nanoparticles-MWCNT; [f]chromium(III) hexacyanoferrate(II); [g]Ni-zeolite/carbon black modified glassy carbon electrode; [h]multiwalled carbon nanotube (MWCNT and cobalt phthalocyanine (CoPc) modified pyrolytic graphite electrode; [i]cobalthexacyanoferrate modified carbon paste electrode; [l]differential pulse voltammetry; [j]nitrogen and sulfur co-doped graphene quantum dot-modified glassy carbon electrode; [k]electrochemical paper-based analytical devices

Repeatability and stability of poly(phenylalanine)/F-MWCNT/GCE

To evaluate the repeatability of the prepared sensor electrode for determining 20 µM VB6, 10 consecutive measurements of 20 µM VB6 were performed using the same electrode. The relative standard deviation (RSD) of the current response was 2.38 %, indicating that the prepared electrode can be used for several measurements to determine VB_6. The electrode fabrication repeatability for VB_6 determination was evaluated by measuring the peak current of 20 µM with four different electrodes prepared under identical conditions. With an RSD of 2.16 %, the outcome demonstrates that all electrodes have essentially identical responses, showing good repeatability of the electrode preparation process. In order to determine the poly (phenylalanine)/F-MWCNT/GCE long-term stability, the current responses to 20 M VB_6 were monitored weekly over one month. The electrode used every week is kept at 4 °C in the refrigerator. The synthesized poly(phenylalanine)/F-MWCNT/GCE was found to have effective long-term stability, as evidenced by the observation that the oxidation current response dropped by 6.3 % at the end of the month.

Robustness study

The robustness of the developed method was examined by studying the effect of small variations of some experimental parameters, such as pH (4.5 ± 0.1), accumulation potential (0.0 ± 0.02 V) and accumulation time (120 ± 2 s) on the recovery of VB_6. As shown in Table 3, the recovery for VB_6

under all studied conditions is in the range of 96.1 – 103.4 %, indicating that small variation of the studied experimental parameters has an insignificant effect on the current response of VB_6. Therefore, the proposed SWV method has good robustness and is reliable for the quantification of VB_6.

***Table 3**. Robustness study for the voltammetric method used for determination of 20 µM VB_6 (n=3)*

Parameters	Mean, µM ± RSD, %	Recovery, %
Optimum values (pH = 4.5, E_{acc} = 0.0 V and t_{acc} = 120 s)	20.68 ± 1.97	103.4
pH (variation)		
4.4	19.42 ± 3.6	97.1
4.6	19.35 ± 1.2	96.8
Accumulation potential (variation)		
0.02 V	19.48 ± 2.63	97.4
-0.02 V	19.22 ± 2.9	96.1
Accumulation time (variation)		
118 s	19.42 ± 1.58	97.1
122 s	19.55 ± 3.8	97.8

Effect of interferents

The impact of potential interfering compounds on the determination of 20 µM VB_6 was examined by SWV under optimal conditions. Except for folic acid (FA), the data demonstrated that none of these interferants at poly(phenylalanine)/F-MWCNT/GCE exhibited a voltammetric response. As can be seen from Figure 11, the response of VB_6 was unaffected by 200− fold excess concentrations of Ca^{2+}, K^+, Mg^{2+}, Cu^{2+}, Fe^{2+}, NO_3^-, CO_3^{2-} and HCO_3^{2-} , 100− fold excess concentrations of ascorbic acid (AA), citric acid (CA), sodium citrate (NaCA), tartaric acid (TA), glucose, fructose, starch, sucrose, caffeine, vitamin B_1 (VB_1), vitamin B_2 (VB_2) and vitamin B_{12} (VB_{12}).

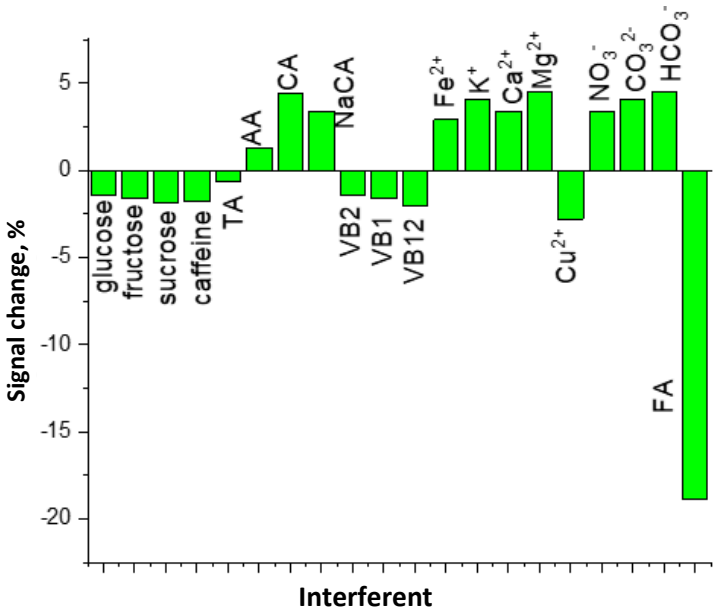

***Figure 11.** Change in peak current response in the presence of different interferents for 20 µM VB_6*

However, FA exhibited two oxidation peaks close to that of VB_6. In the presence of folic acid, even at a concentration ratio of 1:1, the peak current of VB_6 was reduced and the potential shifted to a positive value. Therefore, FA must be separated before the voltammetric measurement of VB_6. Here, however, the examined tablet and beverage samples did not have any folic acid. Additionally, the standard addition method was applied for the quantification of VB_6 to minimize the interference

effect. As a result, the proposed electrode can be successfully utilized to measure VB_6 in pharmaceutical and beverage samples.

Real sample analysis

The developed method was applied for the determination of VB_6 in commercially available pharmaceutical tablets (vitamin B-Complex containing VB_1, VB_6 and VB_{12}) and an energy drink (predatory energy drink). The samples were prepared and diluted to the appropriate concentration with the supporting electrolyte. SWV was used to record signals at poly(phenylalanine)/F-MWCNT/GCE and concentrations of VB_6 were determined by the standard addition method to minimize the matrix effect. As shown in Table 4, the result obtained for VB_6 using the proposed method was found to be 95 mg VB_6/tablet, which is in good agreement with the labelled value of 100 mg VB_6/tablet (relative error 5 %). Similarly, the value of VB_6 in the energy drink was found to be 0.29 mg/100mL, which is close to the labelled amount (0.3 mg/100 mL) (relative error of 3.3 %). Furthermore, recovery studies were carried out by the standard addition method to validate the accuracy and precision of the developed sensor and the results are shown in Table 5. The recovery values varied from 90.0 to 100.4 %, suggesting that the developed method is reliable and effective for the determination of VB_6 in vitamin B-complex and energy drinks without the effect of other constituents of the samples. Furthermore, the low values of RSD (ranging from 0.4 to 4.0 %) indicate good precision of measurements.

Table 4. *Comparison of experimental results with labelled values*

Sample	Labelled content	Experimental content ± SD	Relative error, %
Predatory energy drink	0.3 mg/100 mL	0.29 mg/100 mL ± 0.08	3.3
N-VIT	100 mg/tablet	95 mg/tablet ± 3.1	5.0

Table 5. *Recovery study*

Sample	*C* / μM		RSD, % *n* = 3	Recovery, %
	Added	Found		
N-VIT	0	4.98	3.10	-
	3	7.68	4.00	90.0
	5	9.58	1.30	92.0
	8	12.6	0.37	95.3
	12	17.0	1.80	100.4
Predatory energy drink	0	3.48	2.40	-
	3	6.28	0.26	92.7
	5	8.17	0.95	93.8
	8	10.7	2.90	90.8
	12	15.3	0.40	98.8

Conclusions

In the present study, poly(phenylalanine) and F-MWCNT modified glassy carbon electrode was successfully prepared for the electrochemical determination of VB_6 in pharmaceutical tablet and energy drink samples. The developed sensor exhibits high electrocatalytic activity towards the oxidation of VB_6 due to the synergistic effect between poly(phenylalanine) and F-MWCNT**.** CV study showed that the electrode reaction of VB_6 is the irreversible and adsorption-controlled process. Under the optimized conditions, SWV experiments showed peak currents that increased linearly with VB_6 concentration in two linear ranges (0.5 to 20 and 20 to 200 μM). The detection limit (LOD) was found to be 0.038 μM. The prepared electrode showed high selectivity, stability, repeatability and reproducibility. The acceptable recovery values obtained for VB_6 during real samples analysis

demonstrate that the proposed sensor can be effectively used for the determination of VB_6 in pharmaceutical tablets and energy drinks with high accuracy.

Acknowledgment: *The authors gratefully acknowledge Oromia Education Bureau for the financial support. We are grateful to the Department of Chemistry, Addis Ababa University for providing laboratory facilities.*

Conflicts of Interest: *The authors declare no conflict of interest.*

References

[1] R. Rejithamol, S. Beena, Electrochemical quantification of pyridoxine (VB_6) in human blood from other water-soluble vitamins, *Chemical Papers* **74** (2020) 2011-2020. https://doi.org/10.1007/s11696-019-01049-5

[2] N. Alpar, P. T. Pınar, Y. Yardım, Z. Şentürk, Voltammetric method for the simultaneous determination of melatonin and pyridoxine in dietary supplements using a cathodically pretreated boron-doped diamond electrode, *Electroanalysis* **29** (2017) 1691-1699. https://doi.org/10.1002/elan.201700077

[3] V. Sharma, G. K. Jayaprakas, Fabrications of electrochemical sensors based on carbon paste electrode for vitamin detection in real samples, *Journal of Electrochemical Science and Engineering* **12** (2022) 421-430. https://doi.org/10.5599/jese.1313

[4] E. Dokur, O. Gorduk, Y. Sahin, Cost-effective and facile production of a phosphorus-doped graphite electrode for the electrochemical determination of pyridoxine, *Electroanalysis* **33** (2021) 1657-1667. https://doi.org/10.1002/elan.202100038

[5] T. T. Calam, A novel, efficient and sensitive method for the simultaneous determination of riboflavin (vitamin B2) and pyridoxine hydrochloride (vitamin B_6) in food and pharmacological samples using an electrochemical sensor based on 4, 4'-diamino benzophenone, *Microchemical Journal* **169** (2021) 106557. https://doi.org/10.1016/j.microc.2021.106557

[6] M. Yaman, Determination and evaluation in terms of healthy nutrition of the pyridoxal, pyridoxine and pyridoxamine forms of vitamin B6 in animal-derived foods, *European Journal of Science and Technology* **15** (2019) 611-617. https://doi.org/10.31590/ejosat.540894

[7] S. Z. A. Köseoğlu, Determination and evaluation of the pyridoxal, pyridoxine, and pyridoxamine forms of vitamin B-6 in plant-based foods in terms of healthy vegetarian nutrition, *Progress in Nutrition* **22** (2020) e2020015. https://doi.org/10.23751/pn.v22i3.8509

[8] S. Sel, E. Öztürk Er, S. Bakırdere, Simultaneous determination of niacin and pyridoxine at trace levels by using diode array high-performance liquid chromatography and liquid chromatography with quadrupole time-of-flight tandem mass spectrometry, *Journal of Separation Science* **40** (2017) 4740-4746. https://doi.org/10.1002/jssc.201700933

[9] L. J. Nunez-Vergara, J. A. Squella, J. C. Sturm, H. Baez, C. Camargo, Simultaneous determination of melatonin and pyridoxine in tablets by gas chromatography-mass spectrometry, *Journal of Pharmaceutical and Biomedical Analysis* **26** (2001) 929-938. https://doi.org/10.1016/S0731-7085(01)00447-2

[10] M. J. Chaichi, M. Ehsani, S. Asghari, V. Behboodi, Determination of vitamin B_6 using an optimized novel TCPO–indolizine–H_2O_2 chemiluminescence system, *Luminescence* **29** (2014) 1169-1176. https://doi.org/10.1002/bio.2678

[11] I. Cizmarova, M. Matuskova, O. Stefanik, A. Horniakova, P. Mikus, J. Piestansky, Determination of thiamine and pyridoxine in food supplements by a green ultrasensitive two-dimensional capillary electrophoresis hyphenated with mass spectrometry, *Chemical Papers* **76** (2022) 6235-6245. https://doi.org/10.1007/s11696-022-02309-7

[12] M. Khateeb, B. Elias, F. A. Rahal, Validated spectrophotometric method to Assay of B_6 and B_3 vitamins in pharmaceutical forms using potassium iodide and potassium iodate, *International*

Letters of Chemistry, Physics and Astronomy **60** (2015) 113-119. https://doi.org/10.18052/www.scipress.com/ILCPA.60.113

[13] R. S. Kumar, G. K. Jayaprakash, S. Manjappa, M. Kumar, A. P. Kumar, Theoretical and electrochemical analysis of L-serine modified graphite paste electrode for dopamine sensing applications in real samples, *Journal of Electrochemical Science and Engineering* **12** (2022) 1243-1250. https://doi.org/10.5599/jese.1390

[14] A. Lohrasbi-Nejad, Electrochemical strategies for detection of diazinon, *Journal of Electrochemical Science and Engineering* **12** (2022) 1041-1059. https://doi.org/10.5599/jese.1379

[15] P. S. Ganesh, B. K. Swamy, O. E. Fayemi, E. S. M. Sherif, E. E. Ebenso, Poly (crystal violet) modified pencil graphite electrode sensor for the electroanalysis of catechol in the presence of hydroquinone, *Sensing and Bio-Sensing Research* **20** (2018) 47-54. https://doi.org/10.1016/j.sbsr.2018.08.001

[16] M. C. Monteiro, J. P. Winiarski, E. R. Santana, B. Szpoganicz, I. C. Vieira, Ratiometric electrochemical sensor for butralin determination using a quinazoline-engineered prussian blue analogue, *Materials* **16** (2023) 1024. https://doi.org/10.3390/ma16031024

[17] S. Tajik, Y. Orooji, F. Karimi, Z. Ghazanfari, H. Beitollahi, M. Shokouhimehr, H. W. Jang (2021). High performance of screen-printed graphite electrode modified with Ni–Mo-MOF for voltammetric determination of amaranth, *Journal of Food Measurement and Characterization* **15** (2021) 4617-4622. https://doi.org/10.1007/s11694-021-01027-0

[18] P. Li, Z. Liu, Z. Yan, X. Wang, E. M. Akinoglu, M. Jin, G. Zhou, L. Shui, An electrochemical sensor for determination of vitamin B_2 and B_6 based on AuNPs@ PDA-RGO modified glassy carbon electrode, *Journal of The Electrochemical Society* **166** (2019) B821. DOI 10.1149/2.1281910jes

[19] L. S. Porto, D. N. da Silva, M. C. Silva, A. C. Pereira, Electrochemical sensor based on multi-walled carbon nanotubes and cobalt phthalocyanine composite for pyridoxine determination, *Electroanalysis* **31** (2019) 820-828. https://doi.org/10.1002/elan.201800789

[20] H. Sadeghi, S. A. Shahidi, S. N. Raeisi, A. Ghorbani-HasanSaraei, F. Karimi, Electrochemical determination of vitamin B6 in water and juice samples using an electrochemical sensor amplified with NiO/CNTs and Ionic liquid, *International Journal of Electrochemical Science* **15** (2020) 10488-10498. https://doi.org/10.20964/2020.10.51

[21] G. Tigari, J. G. Manjunatha, Electrochemical preparation of poly (arginine)-modified carbon nanotube paste electrode and its application for the determination of pyridoxine in the presence of riboflavin: an electroanalytical approach, *Journal of Analysis and Testing* **3** (2019) 331-340. https://doi.org/10.1007/s41664-019-00116-w

[22] A. Mekonnen, R. C. Saini, A. Tadese, R. Pal, Square wave voltammetric determination of pyridoxine in pharmaceutical preparations using cobalthexacyanoferrate modified carbon paste electrode, *Journal of Chemical and Pharmaceutical Research* **6** (2014) 544-551.

[23] M. Motaghedifard, M. Behpour, S. M. Ghoreishi, E. Honarmand, Electro-deposition of gold nanostructures on carbon paste electrode: a platform with signal amplification for voltammetric study and determination of pyridoxine (vitamin B_6), *Russian Journal of Electrochemistry* **52** (2016) 477-487. https://doi.org/10.1134/S1023193516050098

[24] G. K. Jayaprakash, R. Flores-Moreno, B. E. K. Swamy, K. Mohanty, P. Dhiman, Pre/post electron transfer regioselectivity at glycine modified graphene electrode interface for voltammetric sensing applications, *Journal of Electrochemical Science and Engineering* **12** (2022) 1001-1008. https://doi.org/10.5599/jese.1438

[25] Z. Guo, G. Wang, J. Li, D. Wu, X. Guo, A miniaturized electrochemical biosensor based on poly (L-threonine) modified pencil graphite electrodes and its application for trace-level determination of uric acid, xanthine and hypoxanthine, *International Journal of Electrochemical Science* **16** (2021) 210262. https://doi.org/10.20964/2021.01.05

[26] P. Naderi, F. Jalali, Poly-L-serine/AuNPs/MWCNTs as a Platform for Sensitive Voltammetric Determination of Progesterone, *Journal of The Electrochemical Society* **167** (2020) 027524. https://doi.org/10.1149/1945-7111/ab6a7f

[27] S. B. Konnur, S. T. Nandibewoor, Electrochemical behavior of 2-Aminothiazole at poly glycine modified pencil graphite electrode, *Analytical and Bioanalytical Electrochemistry* **12** (2020) 208-222.

[28] Y. Zhao, Y. Du, D. Lu, L. Wang, D. Ma, T. Ju, M. Wu, Sensitive determination of vanillin based on an arginine functionalized graphene film, *Analytical Methods* **6** (2014) 1753-1758. https://doi.org/10.1039/C3AY41517A

[29] G. K. Jayaprakash, Pre-post redox electron transfer regioselectivity at the alanine modified nano graphene electrode interface, *Chemical Physics Letters* **789** (2022) 139295. https://doi.org/10.1016/j.cplett.2021.139295

[30] N. Hareesha, J. G. Manjunatha, A simple and low-cost poly (DL-phenylalanine) modified carbon sensor for the improved electrochemical analysis of Riboflavin, *Journal of Science: Advanced Materials and Devices* **5** (2020) 502−511. https://doi.org/10.1016/j.jsamd.2020.08.005

[31] S. K. Revanappa, I. Soni, M. Siddalinganahalli, G. K. Jayaprakash, R. Flores-Moreno, C. Bananakere Nanjegowda, A Fukui analysis of an arginine-modified carbon surface for the electrochemical sensing of dopamine, *Materials* **15** (2022) 6337. DOI: 10.3390/ma15186337

[32] X. Ma, M. Chao, Electrocatalytic determination of maltol in food products by cyclic voltammetry with a poly (l-phenylalanine) modified electrode, *Analytical Methods* **5** (2013) 5823-5829. https://doi.org/10.1039/C3AY41142G

[33] L. Wang, P. Huang, J. Bai, H. Wang, L. Zhang, Y. Zhao, Simultaneous electrochemical determination of phenol isomers in binary mixtures at a poly (phenylalanine) modified glassy carbon electrode, *International Journal of Electrochemical Science* **1** (2006) 403-413.

[34] S. Tahtaisleyen, O. Gorduk, Y. Sahin, Electrochemical determination of tartrazine using a graphene/poly (L-phenylalanine) modified pencil graphite electrode, *Analytical Letters* **53** (2020) 1683-1703. https://doi.org/10.1080/00032719.2020.1716242

[35] M. Chao, X. Ma, Convenient electrochemical determination of sunset yellow and tartrazine in food samples using a poly (L-phenylalanine)-modified glassy carbon electrode, *Food Analytical Methods* **8** (2015) 130-138. https://doi.org/10.1007/s12161-014-9879-6

[36] S. Piña, C. Candia-Onfray, N. Hassan, P. Jara-Ulloa, D. Contreras, R. Salazar, Glassy carbon electrode modified with C/Au nanostructured materials for simultaneous determination of hydroquinone and catechol in water matrices, *Chemosensors* **9** (2021) 88. https://doi.org/10.3390/chemosensors9050088

[37] T. Rohani, M. A. Taher, Novel functionalized multi-walled carbon nanotube-glassy carbon electrode for simultaneous determination of ascorbic acid and uric acid, *Arabian Journal of Chemistry* **11** (2018) 214-220. https://doi.org/10.1016/j.arabjc.2014.12.039

[38] A. M. Díez-Pascual, Chemical functionalization of carbon nanotubes with polymers: a brief overview, *Macromol* **1** (2021) 64-83. https://doi.org/10.3390/macromol1020006

[39] O. Salhi, T. Ez-Zine, L. Oularbi, M. El Rhazi, Electrochemical sensing of nitrite ions using modified electrode by Poly 1, 8-diaminonaphthalene/functionalized multi-walled carbon nanotubes, *Frontiers in Chemistry* **10** (2022) 870393. https://doi.org/10.3389/fchem.2022.870393

[40] G. Tesfaye, N. Negash, M. Tessema, Reduced Graphene Oxide and Poly (phenylalanine) Composite Modified Electrode for the Electrochemical Determination of Vanillin, *Journal of The Electrochemical Society* **169** (2022) 127503. https://doi.org/10.1149/1945-7111/aca561

[41] P. S. Ganesh, B. E. K. Swamy, O. E. Feyami, E. E. Ebenso, Interference free detection of dihydroxybenzene isomers at pyrogallol film coated electrode: A voltammetric

method, *Journal of Electroanalytical Chemistry* **813** (2018) 193-199. https://doi.org/10.1016/j.jelechem.2018.02.018

[42] S. Tajik, H. Beitollahi, A sensitive chlorpromazine voltammetric sensor based on graphene oxide modified glassy carbon electrode, *Analytical and Bioanalytical Chemistry Research* **6** (2019) 171-182. https://doi.org/10.22036/ABCR.2018.89229.1154

[43] P. L. Wang, X. Liu, Q. Q. Hu, H. Gao, W. Ma, Simple and rapid determination of tartrazine using poly (l-arginine)/electrochemically reduced graphene oxide modified glassy carbon electrode, *International Journal of Electrochemical Science* **15** (2020) 8901-8912. https://doi.org/10.20964/2020.09.83

[44] A. B. Monnappa, J. G. Manjunatha, A. S. Bhatt, H. Nagarajappa, Sensitive and selective electrochemical detection of vanillin at graphene-based poly (methyl orange) modified electrode, *Journal of Science: Advanced Materials and Devices* **6** (2021) 415-424. https://doi.org/10.1016/j.jsamd.2021.05.002

[45] S. Jampasa, W. Siangproh, K. Duangmal, O. Chailapakul, Electrochemically reduced graphene oxide-modified screen-printed carbon electrodes for a simple and highly sensitive electrochemical detection of synthetic colorants in beverages, *Talanta* **160** (2016) 113-124. https://doi.org/10.1016/j.talanta.2016.07.011

[46] H. Lian, W. Qian, L. Estevez, H. Liu, Y. Liu, T. Jiang, K. Wang, W. Guo, E. P. Giannelis, Enhanced actuation in functionalized carbon nanotube–Nafion composites, *Sensors and Actuators B: Chemical* **156** (1) (2011) 187-193. https://doi.org/10.1016/j.snb.2011.04.012

[47] X. Liu, L. Luo, Y. Ding, D. Ye, Poly-glutamic acid modified carbon nanotube-doped carbon paste electrode for sensitive detection of L-tryptophan, *Bioelectrochemistry* **82** (2021) 38-45. https://doi.org/10.1016/j.bioelechem.2011.05.001

[48] M. M. Barsan, M. E. Ghica, C. M. Brett, Electrochemical sensors and biosensors based on redox polymer/carbon nanotube modified electrodes: a review, *Analytica Chimica Acta* **881** (2015) 1-23. https://doi.org/10.1016/j.aca.2015.02.059

[49] R. Porada, K. Fendrych, B. Baś, Electrochemical sensor based on Ni-exchanged natural zeolite/carbon black hybrid nanocomposite for determination of vitamin B_6, *Microchimica Acta* **188** (2021) 323. https://doi.org/10.1007/s00604-021-04992-x

[50] E. Laviron , General expression of the linear potential sweep voltammogram in the case of diffusionless electrochemical systems, *Journal of Electroanalytical Chemistry and Interfacial Electrochemistry* **101** (1979) 19-28. https://doi.org/10.1016/S0022-0728(79)80075-3

[51] J. T. Bagalkoti, S. T. Nandibewoor, Modification of glassy carbon electrode by polybromocresol using cyclic voltammetry as a sensor and its analytical applications in determination of pyridoxine hydrochloride in commercial drinks, *Analytical and Bioanalytical Electrochemistry* **10** (2018) 1144-1162.

[52] P. S. Ganesh, S. Y. Kim, D. S. Choi, S. Kaya, G. Serdaroğlu, G. Shimoga, S. H. Lee (2021). Electrochemical investigations and theoretical studies of biocompatible niacin-modified carbon paste electrode interface for electrochemical sensing of folic acid, *Journal of Analytical Science and Technology*, **12** (2021) 47. https://doi.org/10.1186/s40543-021-00301-6

[53] M. M. Barsan, C. T. Toledo, C. M. Brett, New electrode architectures based on poly (methylene green) and functionalized carbon nanotubes: Characterization and application to detection of acetaminophen and pyridoxine, *Journal of Electroanalytical Chemistry* **736** (2015) 8-15. https://doi.org/10.1016/j.jelechem.2014.10.026

[54] D. R. Kumar, D. Manoj, J. Santhanalakshmi, J. J. Shim, Au-CuO core-shell nanoparticles design and development for the selective determination of vitamin B6, *Electrochimica Acta* **176** (2015) 514-522. https://doi.org/10.1016/j.electacta.2015.07.034

[55] S. M. Cottica, J. Nozaki, H. S. Nakatani, C. C. Oliveira, N. E. Souza, J. V. Visentainer, Voltammetric determination of pyridoxine (vitamin B6) in drugs using a glassy carbon

electrode modified with chromium (III) hexacyanoferrate (II), *Journal of the Brazilian Chemical Society* **20** (2009) 496-501. https://doi.org/10.1590/S0103-50532009000300014

[56] E. C. Martins, E. R. Santana, A. Spinelli, Nitrogen and sulfur co-doped graphene quantum dot-modified electrode for monitoring of multivitamins in energy drinks, *Talanta* **252** (2023) 123836. https://doi.org/10.1016/j.talanta.2022.123836

[57] D. F. Pereira, E. R. Santana, A. Spinelli, Electrochemical paper-based analytical devices containing magnetite nanoparticles for the determination of vitamins B_2 and B_6, *Microchemical Journal* **179** (2022) 107588. https://doi.org/10.1016/j.microc.2022.107588